

Repurposing multi-targeting plant natural product scaffolds *in silico* against SARS-CoV-2 non-structural proteins implicated in viral pathogenesis

Von Novi O. de Leon^{1,2}, Joe Anthony H. Manzano^{1,2}, Delfin Yñigo H. Pilapil IV^{1,2}, Rey Arturo T. Fernandez¹, James Kyle Anthony R. Ching^{1,3}, Mark Tristan J. Quimque^{1,4,5}, Kin Israel R. Notarte⁶, and Allan Patrick G. Macabeo^{1*}

¹Laboratory for Organic Reactivity, Discovery and Synthesis (LORDS), Research Center for the Natural and Applied Sciences, University of Santo Tomas, España Blvd., 1015 Manila

²Department of Biological Sciences, College of Science, University of Santo Tomas, Espana Blvd., Manila 1015, Philippines

³Department of Chemistry, College of Science, University of Santo Tomas, Espana Blvd., Manila 1015, Philippines

⁴The Graduate School, University of Santo Tomas, Espana Blvd., Manila 1015, Philippines

⁵Chemistry Department, College of Science and Mathematics, Mindanao State University – Iligan Institute of Technology, Tibanga, 9200 Iligan City, Philippines

⁶Faculty of Medicine and Surgery, University of Santo Tomas, Espana Blvd., Manila 1015, Philippines

*Correspondence:

Phone numbers: +632-3406-1611 extension 4057

Facsimile numbers: +632-8731-4031

E-mail address: apgmacabeo@ust.edu.ph

Abstract:

Background: Accessing COVID-19 vaccines is a challenge despite successful clinical trials. This burdens the COVID-19 treatment gap, thereby requiring accelerated discovery of anti-SARS-CoV-2 agents. Thus, this study explored the potential of anti-HIV reverse transcriptase (RT) phytochemicals as inhibitors of SARS-CoV-2 non-structural proteins (nsps) by targeting *in silico* key sites in the structures of SARS-CoV-2 nsps. Moreover, structures of the anti-HIV compounds were considered for druggability and toxicity. 104 anti-HIV phytochemicals were subjected to molecular docking with papain-like protease (nsp3), 3-chymotrypsin-like protease (nsp5), RNA-dependent RNA polymerase (nsp12), helicase (nsp13), SAM-dependent 2'-O-methyltransferase (nsp16) and its cofactor (nsp10), and endoribonuclease (nsp15). Drug-likeness and ADME (absorption, distribution, metabolism, and excretion) properties of the top ten compounds per nsp were predicted using SwissADME. Their toxicity was also determined using OSIRIS Property Explorer.

Results: Among the twenty-seven top-scoring compounds, the polyphenolic natural products amentoflavone (**1**), robustaflavone (**4**), punicalin (**9**), volkensiflavone (**11**), rhusflavanone (**13**), morelloflavone (**14**), hinokiflavone (**15**), and michellamine B (**19**) were multi-targeting and had the strongest affinities to at least two of the nsps (Binding Energy = -7.7 to -10.8 kcal/mol). Friedelin (**2**), pomolic acid (**5**), ursolic acid (**10**), garcisaterpenes A (**12**), hinokiflavone (**15**), and digitoxigenin-3-O-glucoside (**17**) were computationally druggable. Moreover, compounds **5** and **17** showed good gastrointestinal absorptive property. Most of the compounds were also predicted to be non-toxic.

Conclusions: Twenty anti-HIV RT phytochemicals showed multi-targeting inhibitory potential against SARS-CoV-2 nsp3, 5, 10, 12, 13, 15, and 16, and can therefore be used as prototypes for anti-COVID-19 drug design.

Background:

The rapid spread of the severe acute respiratory syndrome coronavirus 2 (SARS-CoV-2) marks itself as one of the deadliest viruses in recent history due to high mortality and morbidity rates [1, 2]. As of February 2021, the World Health Organization recorded over one hundred and five million cases worldwide with 2.4 million deaths [3]. Continuous efforts are being carried out to unravel the pathophysiology of the virus as well as the pursuit to develop efficacious vaccines and antiviral drugs to combat this pandemic. Recently, several COVID-19 vaccines have been approved for deployment and administration in developed countries. While this presents a step forward towards the mitigation and control of the outbreak, the demand for effective antiviral drugs against SARS-CoV-2 remains irrefutable as promising treatment towards emerging COVID-19 cases. In addition, they may be further developed as therapeutic regimens to subjects with a higher risk of exposure as well as to poor vaccine responders [4, 5].

To develop SARS-CoV-2 targeting drugs, identification of drug targets is essential. SARS-CoV-2 is a betacoronavirus that has an enveloped, positive-sense, single-stranded RNA that encodes structural, non-structural (nsps), and accessory proteins [6]. Among possible drug targets, nsps are highly favored because they function during viral genome replication and post-translational mechanisms which ultimately strengthens virulence and pathogenesis [7]. Although any of the sixteen nsps could be utilized as possible drug targets, the availability of crystal structure along with their vital role in infection, accelerate and enhance the chances of success of anti-COVID-19 drug discovery and development [8].

Natural products are a prolific source of secondary metabolites that are molecular inspirations for drugs, which may have elevated pharmacologic properties and minimal side effects, against viral infections [5, 9-11]. To date, numerous efforts describing the potential of secondary metabolites from various sources as SARS-CoV-2 protein inhibitors especially against

3-chymotrypsin-like cysteine protease (3CL pro) and RNA-dependent-RNA-polymerase (RdRp) have been reported [5, 12-17].

The growing interest to explore the potential of natural products as multi-targeting antagonists of SARS-CoV-2 non-structural proteins led us to repurpose previously reported anti-HIV reverse transcriptase (RT) natural products using molecular docking studies. SARS-CoV-2 and the human immunodeficiency virus (HIV) are single-stranded RNA viruses that utilize RNA-dependent polymerases and code precursor polyproteins vital for their respective pathogenesis. Thus, we computationally interrogated 104 known anti-HIV RT phytochemicals against seven core viral target proteins namely nsp3 (PLpro), nsp5 (3CLpro), nsp12 (RdRp), nsp13 (helicase), nsp15 (endoribonuclease), and nsp16-nsp10 complex (S-adenosylmethionine complex). Drug-likeness as well as the ADMET (absorption, distribution, metabolism, excretion, and toxicity) characteristics of the top-ranked ligands were also predicted to determine their druggability and toxicity risks.

Methods:

Target enzyme preparation

Seven target enzymes with important functions in SARS-CoV-2 infectivity were selected and obtained from the Protein Data Bank (PDB): 3CLpro (PDB ID: 6LU7), PLpro (PDB ID: 6W9C), RdRp (PDB ID: 6M71), helicase (6JYT), nsp 10/16 complex (6W4H), and nsp15 (6VWW). These proteins in three-dimensional structures were added to UCSF Chimera 1.14 platform as PDB files [18]. All proteins belong to SARS-CoV-2 except for helicase due to unavailability of nsp13. Thus, helicase model from SARS-CoV-1 which shares 99.8% sequence identity and 100% sequence similarity with that of SARS-CoV-2 was used [19]. Coronavirus helicase domains are distinct compared to other (+)-sense RNA virus domains due to presence of linkage in a single protein to a binuclear zinc-binding domain at the N-terminus. This domain is composed of 12 conserved cysteine-histidine residues and is a good target in antiviral drug discovery [20-22].

Ligand selection and preparation

A total of 104 plant secondary metabolites (Supplementary Figure 1; Supplementary Table 1) previously reported to inhibit HIV [23] were used as ligands targeting the above-mentioned viral proteins. The plant metabolite structures were formatted as SYBYL mol2 file or in SMILES notation using Avogadro (version 1.20) and were added to the UCSF Chimera 1.14 platform [24].

Molecular docking simulations

Molecular docking experiments were carried out on UCSF Chimera 1.14 platform [18]. Protein structures in three dimensions were opened in PDB formats. Co-crystallized ligands and other molecules were removed from the crystallized protein. Ligands were added in the platform

as SYBYL mol2 files or in SMILES notation. Ligand and protein structures were minimized through addition of missing hydrogen atoms and charges to the structures using the Gasteiger charge method, which was computed using Amber's Antechamber module [25]. 'Flexible ligand into flexible active site' protocol was followed during execution of docking procedures. In this protocol, flexible ligands were allowed and positioned within a grid box which encompasses the enzymatic ligand-binding cavity, as predicted using COACH algorithms [26].

Druggability, ADME, and toxicity prediction

Absorption, distribution, metabolism and excretion (ADME) properties of top twenty-seven compounds were computationally predicted using SwissADME software. Evaluation of pharmacokinetic profiles of compounds were performed according to Lipinski's 'rule of five' which assesses biochemical properties of a drug candidate involved in permeation and cell absorption. Three of the following values need to be met according to Lipinski's criteria: <500 Daltons (Da) for molecular weight, <5 for calculated lipophilicity (Log P), <10 for the number of hydrogen-bond acceptors, and <5 for the number of hydrogen bond donors [27]. Moreover, toxicity of hit compounds, specifically mutagenicity, tumorigenicity, reproductive toxicity, and irritant effects, were predicted in silico using OSIRIS Property Explorer software [28][16]. Solubility (Log S) was also predicted using the same software in which $\text{Log S} \geq -4$ indicates good solubility and favorable absorption of compounds.

Results:

Target enzymes

The targeted nsps were classified according to their major functions in the SARS-CoV-2 life cycle, specifically autolytic processing, viral replication, and host immunity evasion. The cysteine proteases, PLpro and 3CLpro, function in the proteolytic cleavage of the replicase polyproteins into individual nsps. RdRp and helicase are components of the replication-transcription complex vital for SARS-CoV-2 proliferation. The SAM-dependent 2'-O-methyltransferase in complex with nsp10 as its cofactor provides a 5' cap to the RNA genome through C2'-O-methyl-ribosyladenine, conferring RNA stability and host cell immunity protection. Lastly, the endoribonuclease hinders recognition of dsRNA intermediates by host dsRNA sensors.

Ligand selection and molecular docking

104 repurposed anti-HIV reverse transcriptase phytochemicals against SARS-CoV-2 nsps comprised of polyphenolics, terpenoids, alcohols, and alkaloids were docked with nsps3, 5, 10, 12, 13, 15, and 16. Twenty-seven compounds showed favorable binding affinities while twenty exhibited multi-targeting properties (Figure 1).

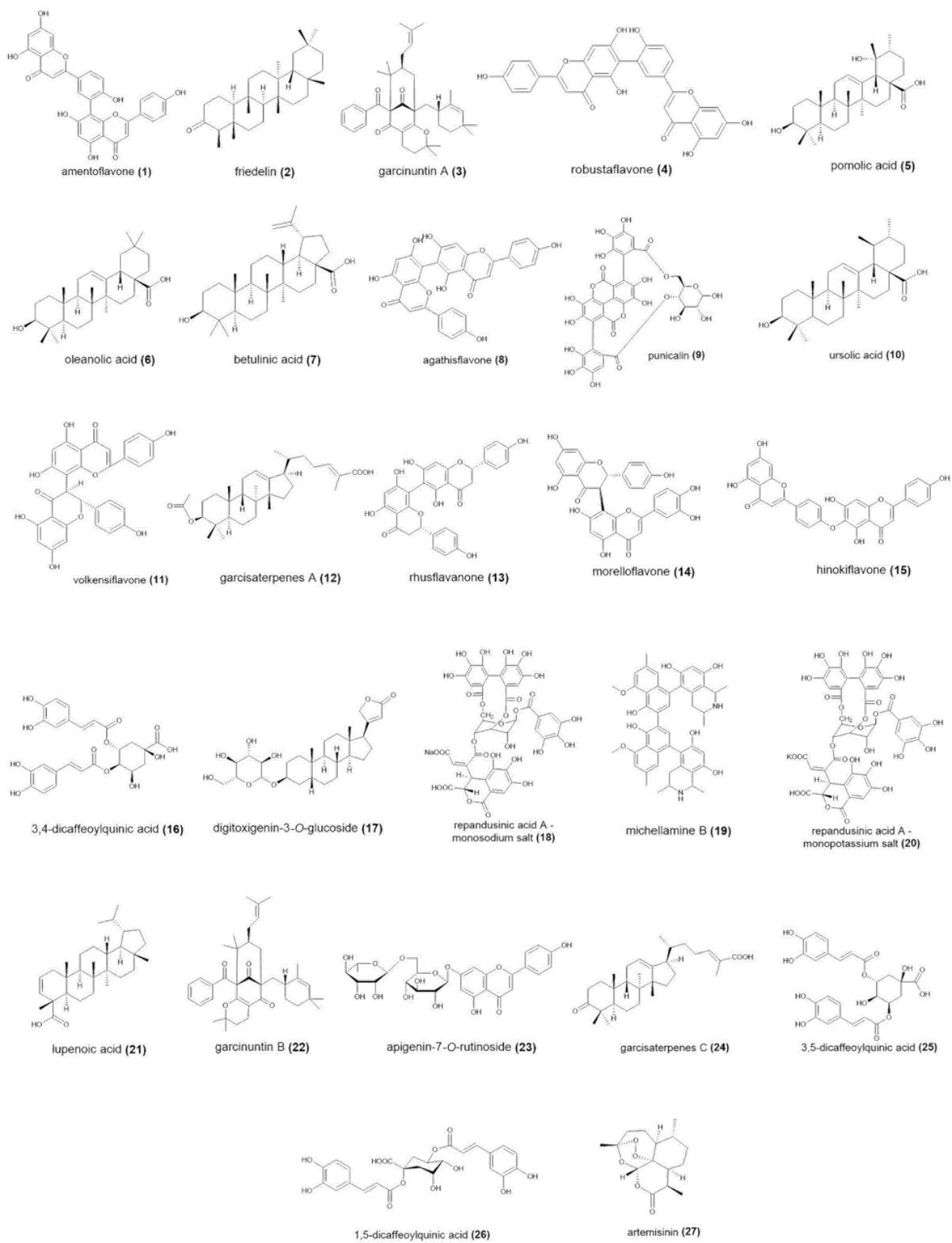


Figure 1 Anti-HIV RT phytochemicals with strong binding affinities to at least one of the target nsps

Molecular docking with autolytic-processing enzymes (nsp3 and nsp5)

Top ten compounds against PLpro exhibited binding affinities of -10.1 to -10.8 kcal/mol, which is relatively stronger compared to the binding energy (BE) of -6.9 kcal/mol of the reference drug, lopinavir [16] (Table 1). The biflavonoid amentoflavone (**1**) exhibited highest affinity to PLpro with its benzopyrone (ring C) and phenolic moiety (ring B) participating through H-bonding and *pi*-anion interactions with Lys711, respectively (Figure 2A). Ring C additionally bound Ile580 through *pi*-alkyl interaction. The phenolic functionality in ring B also participated in hydrogen bonding with His342 and in *pi*-alkyl binding with Ala579 and Leu742. Ring A' of the benzopyrone moiety bound Arg712 by H-bonding and Ile310 by *pi*-alkyl interaction. Meanwhile, the phenolic moiety (ring B') exhibited *pi*-anion interaction with Asp339 and *pi*-cation interaction with Arg558.

On the other hand, top-ranked ligands against 3CLpro exhibited binding affinities of -7.9 to -8.6 kcal/mol, which is stronger than the BE of -7.6 kcal/mol of lopinavir [16] (Table 1). The biflavones amentoflavone (**1**) and volkensiflavone (**11**) showed highest affinity to 3CLpro (Figure 2B). The chromanone moieties (rings A' and C) of amentoflavone showed stacked amide-*pi* and *pi*-*pi* T-shaped interactions with His41, a component of the 3CLpro catalytic dyad. These interactions were also demonstrated by its phenolic moiety to Asn142. The chromanone moiety (rings A and C) was bound to Met165 through *pi*-alkyl interaction along with hydrogen bonds with Val186, Arg188, and Glu166. Ring A' also bound Cys44 through H-bonding. Volkensiflavone (**11**) was likewise bound to the 3CLpro catalytic dyad, His41 and Cys145, through *pi*-anion interaction and hydrogen bonding of the chromanone moieties (rings C and A' respectively). Moreover, rings A' of the flavone substructure also exhibited hydrogen bonding with Glu166 while the B ring residue bound Thr25 through a *pi*-sigma interaction.

Table 1 Binding affinities and interactions of top ten ligands against the cysteine proteases

Target	Cpd	Binding affinity	Hydrogen bonds	Other interactions
PLpro	1	-10.8	His342, Lys711, Arg712	Lys711, Asp339, Arg558, Ile310, Ile580, Ala579, Leu742
	2	-10.7	None	His342, Leu557, Ala579, Leu742
	3	-10.7	Lys711, Arg712	Ile310, Ala338, His342, Leu557, Ala579, Ile580, Val635, Lys694, Arg712
	4	-10.6	Thr583, Arg586, Tyr634	Asp339, Arg558, Ala579, Ile580, Met630, Leu742
	5	-10.4	Val659	Leu557, Arg558, Met560, Ala579, Ile580, Leu742
	6	-10.3	Asp226	None
	7	-10.2	Lys711, Arg712	None
	8	-10.2	Asp339, Arg586, Tyr634	Val304, Ala338, Asp339, Arg558, Ala579, Lys711, Leu742
	9	-10.2	Gly337, Asp339, Arg345, Arg558, Arg712	Ile310
	10	-10.1	Asp339, Arg345, Tyr634	Leu557, Ile580, Met630, Val635, Lys711, Leu741
3CLpro	1	-8.6	Cys44, Val186, Arg188, Glu166	Thr25, His41, Asn142, Cys145, Met165
	11	-8.6	Cys145, Glu166	Thr25, His41
	12	-8.5	Thr24, Ser46, Thr190, Gln192	Thr25, His41
	13	-8.5	Thr26, His41	Met49, Pro168
	4	-8.5	Arg188, Gln189	None
	8	-8.4	Thr26, Gln189, Thr190	Leu27, Met49, Glu166, Met165, Pro168
	14	-8.4	Phe140, Gly143, Arg188, Gln189	His41
	15	-8.1	Asn119, Val186	None
	16	-7.9	Gly143, Cys145, Glu166, Gln189	His41, Gln189
	17	-7.9	His41, Asn119	His41, Gly143, His163
	3	-7.9	His41	Leu27, His41

Molecular docking with replication-transcription complex enzymes (nsp12 and nsp13)

Among the top ten compounds against RdRp with binding affinities of -8.6 to -9.5 kcal/mol, the ellagitannin punicalin (**9**) exhibited the highest affinity (Table 2; Figure 3A). This BE is lower than -7.6 kcal/mol of the reference drug favipiravir [16]. The ellagic acid moiety occupied Ile494 and its galloyl hydroxyl bound Asn497, which are both components of the RdRp finger domain that is responsible for the entry and exit of the RNA template during replication-transcription [29]. Moreover, its glucose hydroxyl and hydrogen participated in hydrogen bonding and carbon-hydrogen bonding respectively with Asp684, a component of the motif B of the polymerase active site [30]. Other interactions include the participation of its ellagic acid moiety in *pi*-alkyl interaction with Lys577, galloyl hydroxyl in hydrogen bonding with Gly590, carbonyl oxygen in hydrogen bonding Tyr689, and glucose moiety in carbon-hydrogen bonding with Ala685.

Meanwhile, the top-ranked ligands against helicase had binding affinities of -8.4 to -9.2 kcal/mol in which the biflavonoids rhusflavanone (**13**) and morelloflavone (**14**) exhibited the strongest affinity, comparable to the reference drug cepharanthine with BE of -10.3 kcal/mol [31] (Figure 3B). Compound **13** occupied the helicase Rec1A domain, which is a component of the nucleotide binding site, through hydrogen bonding of its chromanone (ring A') hydroxyl and pyrone (ring C') oxygen with Lys288 and Ala316, respectively [31]; *pi*-alkyl interactions of its chromene moieties, rings A with Ala316 with Ala316 and ring A' with Lys320; and *pi*-cation interaction of its hydroxyphenyl moiety (ring B) with Lys320.

Table 2 Binding affinities and interactions of top ten ligands against the nsps vital for replication

Target	Cpd	Binding Affinity	Hydrogen bonds	Other interactions	
RdRp	9	-9.5	Asn497, Gly590, Asp684, Tyr689	Ile494, Lys577, Asp684, Ala685	
	10	-9.1	Val495	Ile494, Lys577, Ala580, Ala685	
	2	-8.9	None	Ile494, Arg569, Leu576, Lys577, Ala685	
	15	-8.9	Asn496, Asn497, Arg569, Ala685	Ile494, Lys500, Lys577, Ala580, Ala685	
	18	-8.9	Asn496, Arg569, Ala685, Ser759	Lys545, Arg569	
	19	-8.8	Ile548, Lys593, Ser814	Ile548, Lys593, Leu758, Asp761, Cys813, Pro832, Arg836, Ile837, Ala840	
	20	-8.8	Ile494, Asp684	Lys500, Lys545, Arg569, Ser682	
	4	-8.8	Asn497, Arg569	Ile494, Lys500, Arg569, Lys577, Ala685	
	21	-8.7	None	Ile494, Lys500, Leu576, Lys577, Ala685, Tyr689	
	1	-8.6	Asn497, Asp684	Arg569, Ala580, Ala688, Tyr689	
	3	-8.6	Arg569, Gln573	Ile494, Lys500, Lys577, Ala580, Ile589, Ala685, Ala688, Tyr689	
	5	-8.6	Arg569, Gln573	Leu576, Lys577, Ala580, Ala685	
	Helicase	14	-9.2	Glu341, Asp534	Ala312, Ala313, Val340
		13	-9.2	Lys288, Ala316, Arg443	Thr286, Ala316, Lys320, Gly538, Ser539
		15	-9	Arg332, Glu319, Cys342, Ser310, Asp534	Met378, Ala312, Ala316, Asp315
8		-8.9	Gly285, Ala316, Ser289, Lys288, Glu375, Gln537	Ala312, Lys320, Gln537	
4		-8.9	Gly285, Lys288	Arg443, Arg442, Glu540, Lys320, Ala316, Ala312, Ala313	
19		-8.7	None	Gly538, Glu319, Glu540, Ala316, Ser535, Ala312, Ala313	
1		-8.6	None	Ala312, Cys342, Asp315, Ala316, His311	
22		-8.6	Asn459	Phe437, Lys460, Pro434, Gly433, Lys430, Pro402, Tyr457, Ala403	
23		-8.5	Lys430, Gln281, Val456, Tyr457	Phe437, Pro434, Lys430, Leu455	
24	-8.4	Leu417, Asn557, Asn516	Phe422, Pro406, Pro408		

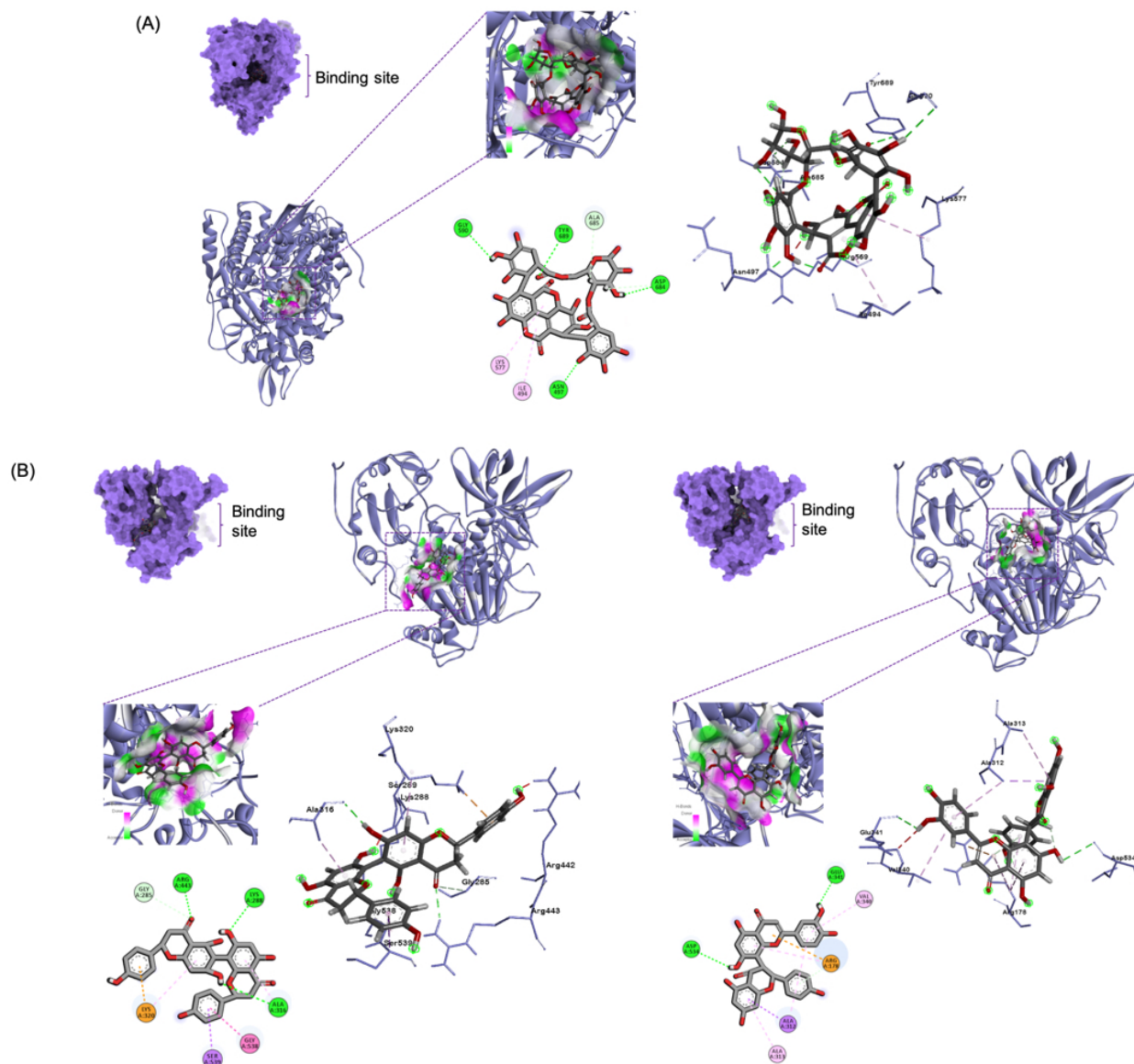


Figure 3 Top 1-binding compounds in complex with their target enzymes vital in replication: (A) punicalin (9) in complex with RdRp, (B) rhusflavanone (13) (left) and morelloflavone (14) (right) bound to helicase

Compound **13** also occupied the Rec2A domain of the nucleotide binding site through a hydrogen bond of its pyrone (ring C) carbonyl with Arg443, an amide- π stacked interaction of its hydroxyphenyl moiety (ring B') with Gly538, and a π -sigma interaction of ring B' with Ser539. A pyrone (ring C) carbonyl further contributed to the binding affinity of compound **13** by binding to Thr286 through van der Waals forces. On the other hand, a dihydroxyphenyl moiety (ring B') of compound **14** bound Glu341 through hydrogen bonding and both Ala312 and Val340 by π -alkyl interactions. Ring A of its chromanone functionality bound Ala313 through a π -alkyl interaction and also Ala312 by π -sigma interaction. These residues are members of the helicase Rec2A domain of the nucleotide binding site. In addition, a benzopyrone hydroxyl (ring A') of compound **14** bound Asp 534, which is a residue of the Rec1A helicase domain of the nucleotide binding site.

Molecular docking with enzymes functioning in the evasion of host immunity

SAM-dependent 2'-O-methyltransferase complex enzymes (nsp10/nsp16 complex)

Top compounds against nsp16 exhibited affinities from -9.3 to -10.6 kcal/mol. The SAM-binding site was targeted and the biflavonoid robustaflavone (**4**) and the alkaloid michellamine B (**19**) demonstrated the greatest affinity compared to the reference drug antrafenine with BE of -10.3 kcal/mol [32] (Table 3; Figure 4A). Hydroxyphenyl ring B of compound **4** exhibited π -alkyl interactions with Leu6898 and Met6929, and a hydrogen bonding with Cys6913. The hydroxyphenyl ring B' showed carbon-hydrogen bonding with Asn6841. Moreover, its benzopyrone moiety (rings A and C) was in π -anion interaction with Asp6897 and its chromene hydrogen was in hydrogen bonding with Asp6928. A van der Waals force interaction between its pyrone ring C oxygen and Gly6869 was also observed.

Table 3 Binding affinities and interactions of top ten ligands against the nsp5 of the SAM-dependent 2'-O-methyltransferase complex

Target	Cpd	Binding affinity	Hydrogen bonds	Other interactions
nsp16	19	-10.6	Asp6897, Asp6928	Cys6913, Cys6914, Met6929, Asp6931, Phe6947, Gly6869, Leu6898
	4	-10.6	Lys6844, Cys6913, Asp6928, Asp6928, Asn6996	Asn6841, Asp6897, Gly6869, Met6929, Leu6898, Glu7001
	1	-10.2	Asn6841, Asp6897, Leu6898, Asp6912	Pro6932, Asp6897, Leu6898, Met6929, Phe6947
	23	-10.2	Asp6931, Cys6913, Tyr6930	Asp6931, Phe6947, Asp6912, Leu6898, Met6929, Asp6897, Gly6869, Asp6928
	25	-9.5	Gly6911, Asp6873, Gly6871, Tyr6930	Leu6898, Cys6913, Met6929, Tyr6930,
	3	-9.5	Asn6841, Lys6844, Asn6996	Met6839, Met6840, Tyr6930, Pro6932, Ser6999
	18	-9.5	Asn6841, Asp6897, Asn6899, Tyr6930, Asn6996, Ser6999, Glu7001	Lys6844, Lys6968
	13	-9.5	Ser759, Asp761	Leu758, Ala688, Asp760, Cys813
	26	-9.4	Asn6899, Asp6873, Lys6844, Asn6841, Asp6928, Leu6898, Asp6912	Cys6913, Phe6947, Gly6869, Tyr6930, Asp6897,
	20	-9.3	Lys6844, Gly6869, Asp6873	Lys6935
nsp10	4	-7.7	Asp4335	Arg4331, Ile4334, Lys4346
	1	-7.4	His4333, Ile4334	Arg4331
	27	-7.3	Asp4344, Leu4345	Tyr4329, Cys4327, His4336, Pro4337, Leu4345, Leu4365
	15	-7.3	Arg4331, His4333, Lys4348, Gly4323, Tyr4349	Val4295, Gly4322, Ala4324
	19	-7.2	Lys4346	Cys4330, His4333, Ala4324, Lys4346, Val4295
	11	-7.2	Asn4293	Cys4294, Lys4296, Val4295, Leu4298
	23	-7.1	Cys4330, His4333, Ile4334, Asp4335, His4336	Lys4346
	25	-7	Tyr4329, His4333, Ala4324, Leu4345, Lys4348	Lys4346, Tyr4349
	8	-7	Cys4343	Lys4346, Gly4347, Phe4342
	26	-6.9	Leu4345, Lys4348, Gly4347, Ala4324, His4333, Ile4334, Tyr4329	Lys4348, Arg4331, Lys4346,
17	-6.9	Tyr4329, His4336	Asn4293, Arg4331, Ala4324, His4333, Lys4346, Ile4334	
9	-6.9	Ala4324, Lys4346, Lys4348, Tyr4349	Val4295, Gly4322, Gly4347, Ala4324, Tyr4349	
20	-6.9	Leu4345, Gly4347, Lys4348	Ala4324, Arg4331, His4333	

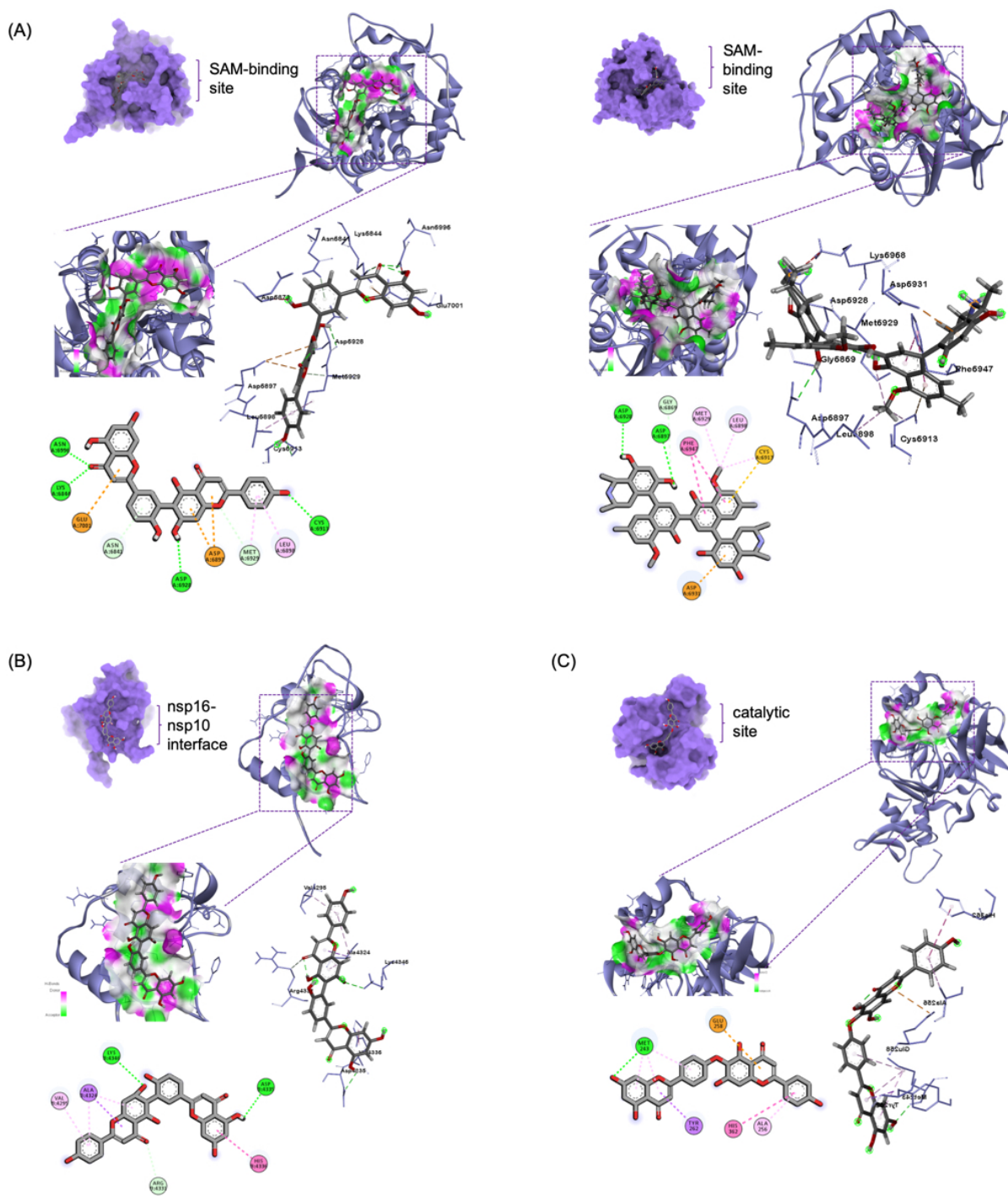


Figure 4 Top 1-binding compounds in complex with nsps involved in host immunity evasion: (A) robustaflavone (**4**) (left) and michellamine B (**19**) (right) complexed with S-adenosylmethionine-dependent 2'-O-methyltransferase, (B) robustaflavone (**4**) bound to nsp10, and (C) hinokiflavone (**15**) bound to nsp15

Another pyrone moiety (ring C') also interacted with nsp16 through a *pi*-anion interaction with Glu7001. Lys6844 and Asn6996 were occupied by the pyrone ring C' carbonyl through hydrogen bonding. On the other hand, compound **19**'s isoquinoline moiety was in H-bonding with Asp6928 and Asp6897 and in carbon-hydrogen bonding with Gly6869. Another isoquinoline moiety was in *pi*-anion interaction with Asp6931. Moreover, a naphthalene moiety participated in *pi*-*pi* T-shaped interaction with Phe6947 and in *pi*-sulfur interaction with Cys6914. A methyl group connected to naphthalene manifested alkyl interactions with Met6929, Leu6898, and Cys6913.

In connection, top compounds against nsp10 showed binding affinities of -6.9 to -7.7 kcal/mol comparable to the -8.5 kcal/mol BE of siramesine [32]. The interface between nsp10 and nsp16 was targeted and several interactions were observed. Biflavonoid robustaflavone (**4**) had the highest affinity (Figure 4B). Its pyrone ring C' was in carbon-hydrogen bonding with Ile4334. Chromanone (ring A') hydroxyl formed H-bonding with Asp4335. Carbon atoms of chromanone (rings A and C) and hydroxyphenyl ring B' formed salt bridges with Lys4346 while ring C' carbonyl exhibited a salt bridge with Arg4331.

Endoribonuclease (nsp15)

Top-scoring compounds against nsp15 exhibited affinities of -8.6 to -7.3 kcal/mol, compared to that of the reference nitrogenous inhibitor, Z16215674, with -9.07 kcal/mol [33] (Table 4). The biflavonone hinokiflavone (**15**) scored the highest affinity, noting its interactions with its putative binding site that is proximal to the catalytic triad of His235, His250, and Lys290: flavone moiety (rings A, B, and C) in hydrogen bonding and *pi*-alkyl interaction with Met243, pyrone ring C in *pi*-sigma interaction with Tyr262, pyrone ring C' in *pi*-anion interaction with Glu258, and hydroxyphenyl ring B' in *pi*-alkyl and *pi*-*pi* stacked interactions with Ala256 and His362, respectively (Figure 4C).

Table 4 Binding affinities and interactions of top ten ligands against nsp15

Target	Cpd	Binding affinity	Hydrogen bonds	Other interactions
nsp15	15	-8.6	Met243	Met243, Tyr262, Glu258, His362, Ala256
	4	-8.5	None	Lys281, Glu285, Tyr262, Met243
	1	-8.4	Gly254	Met243, Ala256, Glu258
	25	-8.1	Phe265, Ser266	Lys281, Ser266, Ala256
	23	-8	None	Glu258, Ala256, Gly263, Asp264, Phe265
	26	-7.8	Glu285, Glu364	Ala256, Ser266, Met243, Lys281, Glu285
	12	-7.7	Glu285	Ala256, Met243, Tyr262, Lys281
	14	-7.7	Arg282	Glu285, Lys281, Phe265
	13	-7.3	Gly263, Asp264	Ala256, His259, Asp264, Met243, Glu285
	17	-7.3	Glu258	None

Druggability, ADME, and Toxicity

Six of the 20 top-scoring and multi-targeting repurposed phytochemicals were found to be druggable according to Lipinski's rule of five (Table 5). Hinokiflavone (**15**) is a top-scoring, multi-targeting, druggable compound. Moreover, compounds **5** and **17** were multi-targeting and exhibited good gastrointestinal absorption property.

In addition, compounds **25** and **26** showed the best solubility in water of -2.85, thereby depicting good excretion properties (Table 6). Toxicity prediction through OSIRIS Property Explorer showed that all top compounds except **11**, **14**, **15**, **18**, **19**, and **20** have no mutagenic, tumorigenic, irritant, and reproductive toxicity risks (Table 6).

Table 5 Druggability of top, multi-targeting compounds according to Lipinski's rule of five

Cpd	MW <500	#H-bond acceptors <10	#H-bond donors <5	Lipophilicity MLogP<5	Lipinski violations	Drug- likeness	Target
1	538.46	10	6	0.25	2	No	PLpro, 3CLpro, RdRp, helicase, nsp10, nsp16, nsp15
2	426.72	1	0	6.92	1	Yes	PLpro, RdRp
3	570.8	4	0	5.03	2	No	PLpro, 3CLpro, RdRp, nsp16
4	538.46	10	6	0.25	2	No	PLpro, 3CLpro, RdRp, helicase, nsp10, nsp16, nsp15
5	472.7	4	3	4.97	1	Yes	PLpro, RdRp
8	538.46	10	6	0.25	2	No	PLpro, 3CLpro, helicase, nsp10
9	782.53	22	13	-2.56	3	No	PLpro, RdRp, nsp10
10	456.7	3	2	5.82	1	Yes	PLpro, RdRp
11	540.47	10	3	0.41	2	No	3CLpro, nsp10
12	498.74	4	1	5.97	1	Yes	3CLpro, nsp15
13	542.49	10	6	0.58	2	No	3CLpro, helicase, nsp16, nsp15
14	556.47	11	7	-0.08	3	No	3CLpro, helicase, nsp15
15	538.46	10	5	0.52	1	Yes	3CLpro, RdRp, helicase, nsp10, nsp15
17	520.65	8	4	1.95	1	Yes	3CLpro, nsp10, nsp15
18	992.64	28	14	-3.39	3	No	RdRp, np16
19	756.88	10	8	3.18	2	No	RdRp, helicase, nsp10, nsp16
20	1008.75	28	14	-3.39	3	No	RdRp, nsp10, nsp16
23	578.52	14	8	-2.96	3	No	helicase, nsp10, nsp16, nsp15
25	516.45	12	7	-0.35	3	No	nsp10, nsp16, nsp15
26	516.45	12	7	-0.35	3	No	nsp10, nsp16, nsp15

Table 6 Toxicity risks of top, multi-targeting compounds as predicted by OSIRIS Property Explorer

Cpd	Toxicity Risk				Solubility (LogS)
	Mutagenic	Tumorigenic	Irritant	Reproductive effective	
1	No	No	No	No	-6.16
2	No	No	No	No	-6.97
3	No	No	No	No	-7.66
4	No	No	No	No	-6.18
5	No	No	No	No	-5.66
8	No	No	No	No	-6.18
9	No	No	No	No	-5.89
10	No	No	No	No	-6.11
11	No	No	No	High Risk	-5.11
12	No	No	No	No	-6.37
13	No	No	No	No	-5.75
14	No	No	No	High Risk	-4.82
15	No	No	No	High Risk	-6.69
17	No	No	No	No	-4.42
18	No	No	High Risk	No	-3.54
19	No	High Risk	No	No	-11.38
20	No	No	High Risk	No	-3.54
23	No	No	No	No	-2.95
25	No	No	No	No	-2.85
26	No	No	No	No	-2.85

Discussion:

The exploration of the SARS-CoV-2 genome revealed viral enzymes that can be targeted to combat COVID-19. Aside from the structural proteins including the spike and envelope proteins, SARS-CoV-2 pathogenesis requires non-structural proteins that can be targeted due to their functions in post-translational processing, replication, and host immunity evasion [34]. The targeted nsps were PLpro, 3CLpro, RdRp, helicase, SAM-dependent 2'-O-methyltransferase and its cofactor (nsp10), and the endoribonuclease. The understanding of these nsps requires knowing the fate of the SARS-CoV-2 genome after it is released into the host cell. The open reading frames 1a and 1ab genes at the 5'-end of the genome are translated into polyproteins pp1a and pp1ab, which contain nsps 1-10 and nsps 1-16, respectively [35]. PLpro and 3CLpro are mainly involved in post-translational processing through the autolytic cleavage of the polyproteins wherein PLpro cleaves 3 sites at the N-terminus while 3CLpro cleaves through the remaining sites (11 sites in pp1ab) to release the nsps [34] (Figure 5).

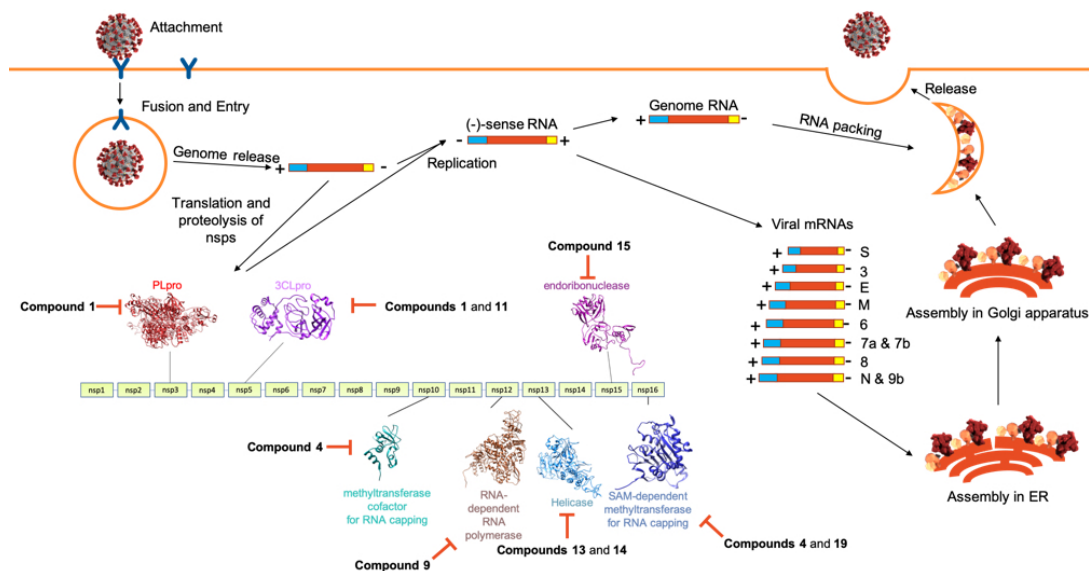


Figure 5 The SARS-CoV-2 life cycle highlighting the role of nsps in replication and transcription and the potential inhibited target SARS-CoV-2 nsps of repurposed anti-HIV RT phytochemicals.

SARS-CoV-2 virion image credit: CDC/ Alissa Eckert (MSMI) and Dan Higgins (MAMS)

These cysteine proteases were included in this study, although these are widely established targets [36, 37], in order to provide a full picture of the infective mechanisms provided by nsps from autolytic processing to replication-transcription and genome modifications in SARS-CoV-2. Their inclusion also highlights the multi-targeting capacity of the tested compounds against the nsps. Proceeding to replication-transcription, the replication-transcription complex which is notably composed of RdRp and helicase replicates the positive-sense genome into a negative-sense RNA genome that serves as the template for the subsequent replication of the new positive-sense genome and the transcription of viral subgenomic mRNAs that are further translated into structural and accessory proteins [38]. In this complex, RdRp elongates the daughter strand through the polymerization of nucleotides, while helicase clears RNA secondary structures and RNA-binding proteins [39]. In addition, among those targeted nsps in this study, the complex of SAM-dependent C2'-O-methyltransferase (nsp16)—that is specific to methylguanine-triphosphate-adenosine—and nsp 10 as its cofactor confer host immune evasion properties for SARS-CoV-2 due to the cap methylation of viral mRNAs [40]. Similarly, the endoribonuclease (nsp15) cleaves at the 3' end of uridylylates[41] and also antagonizes the activation of host dsRNA sensors [42], thereby eluding host immunity. Our results, therefore, highlighted the role of anti-HIV RT phytochemicals as potential antagonists of SARS-CoV-2 by interfering with the functionality of these nsps.

With known targets in the SARS-CoV-2 pathogenesis, discovery of therapeutic agents is possible amidst the unavailability of laboratory-based high throughput screening experiments. This endeavor is accelerated by computer-aided drug discovery through virtual screening which offers a structural approach that focuses on key residues vital in the functioning of the target enzyme [43]. Thus, this removes the trial-and-error, random screening and provides primary direction through lead compounds for drug development [16]. In connection with this efficiency, the repurposing of established anti-HIV compounds led to the discovery of new anti-SARS-CoV-

2 compounds. The repurposing of anti-HIV RT phytochemicals against SARS-CoV-2 is an opportunistic approach on the basis that both SARS-CoV-2 and HIV are positive-sense RNA viruses that rely on RNA-dependent polymerases—SARS-CoV-2 RdRp and HIV reverse transcriptase—for their incorporation into the host cell machinery and encode polyproteins—replicase polyprotein 1a and 1ab for SARS-CoV-2 and Gag and Gag-Pol polyproteins for HIV—that contain functional enzymes and structures vital for their development to a mature virion. Enzymes in the HIV Gag-Pol polyprotein include the viral protease that cleaves the polyproteins and reverse transcriptase that reversely transcribes the RNA genome into DNA for host cell integration [44]. As previously discussed, this is similar to SARS-CoV-2 polyproteins that contain the nsps.

The repurposing of established anti-HIV compounds means that the lead compounds in this study can be easily obtained from previously explored plants. This is in consideration of the fact that despite the successful formulation and clinical trials of vaccines, not all countries can swiftly procure and distribute vaccines to their population [45]. Vaccine percent efficacies imply that populations can still be infected, thereby highlighting the need for continuous anti-COVID-19 drug development. Since some of these plant sources are consumed by populations, the top 1 multi-targeting compounds may be taken in by people around the world. Amentoflavone (**1**) can be obtained from the Chinese olive fruit, *Canarium album* [46]. Robustaflavone (**4**) can be obtained from the leaves of *Garcinia epunctata*, which is used in Cameroon folk medicine [47]. Punicalin (**9**) can be obtained from the peel of pomegranate, *Punica granatum* [48]. Volkensiflavone (**11**) and morelloflavone (**14**) can be obtained from the seeds and rinds of *Garcinia intermedia* [49]. Rhusflavanone (**13**) can be obtained from the fruit of *Searsia parviflora* [50]. Hinokiflavone (**15**) can be obtained from *Selaginella tamariscina* [51]. Lastly, michellamine B (**19**) can be obtained from the leaves of *Ancistrocladus korupensis* [52]. The multi-targeting potential of compounds increases the chance of getting a maximal inhibitory effect [53]. Although

most of these top 1 compounds were predicted *in silico* to be non-druggable, efforts are rising to explore compounds in the oral druggable space beyond the rule of five (bRo5) [54, 55] and these can still serve as templates for drug design or even undergo *in vitro* assays for validating their anti-SARS-CoV-2 properties. Additionally, four of these did not manifest toxicity *in silico*. The biflavonoids volkensiflavone (**11**), morelloflavone (**14**), and hinokiflavone (**15**) were computationally predicted as non-mutagenic, non-tumorigenic and non-irritant, but were predicted to pose reproductive toxicity risk which may be attributed to their chromene and hydroxyphenyl moieties. It should be noted, however, that hinokiflavone (**15**) is the only druggable top 1 compound. Michellamine B (**19**) was also predicted to be tumorigenic due to its naphthalene moiety. Nevertheless, these can still serve as drug templates considering the consumption of their plant sources among populations and their inhibitory interactions with their target nsps. In addition, compounds **5** and **17** exhibited good gastrointestinal absorptive feature as implicated by their favorable lipophilicity and polar surface area [56]. Moreover, these did not manifest any form of toxicity *in silico*.

Conclusions:

The search for anti-COVID-19 therapeutic agents is a response to the continuous spread of the virus amidst vaccine availability. The similarity between the pathogenesis of HIV and SARS-CoV-2 inspired the repurposing of previously reported anti-HIV reverse transcriptase phytochemicals against SARS-CoV-2 nsps implicated in viral replication, post-translational processing and host immunity evasion mechanisms. The top-ranking polyphenolics, terpenoids and alkaloid identified in this study can be further screened using confirmatory *in vitro* and *in vivo* assays, and can serve as prototypes for designing novel anti-COVID-19 drugs. As promising drug templates, functionalities in the compound structure can be modified to improve druggability and pharmacokinetic properties.

List of Abbreviations:

3CLpro: 3-chymotrypsin-like protease; ADME: Absorption, digestion, metabolism, and excretion; BE: Binding energy; COVID-19: Coronavirus disease 2019; Cpd: compound; dsDNA: double-stranded DNA; HIV: Human immunodeficiency virus; kcal/mol: Kilocalorie/mole; nsp: Non-structural protein; PDB: Protein data bank; PLpro: Papain-like protease; RdRp: RNA-dependent RNA polymerase; RNA: Ribonucleic acid; RT: Reverse transcriptase; SARS-CoV-2: Severe acute respiratory syndrome coronavirus 2

References

- [1] Albano PM, Notarte KI, Macaranas I, Maralit B (2020) Cross-contamination in molecular diagnostic laboratories in low-and middle-income countries. *Philipp J Pathol* 5: 7-11.
doi:10.21141/PJP.2020.09
- [2] Viswanathan T, Arya S, Chan SH, Qi S, Dai N, Hromas RA, Park JG, Oladunni F, Martinez-Sobrido L, Gupta YK (2020) Structural Basis of RNA Cap Modification by SARS-CoV-2 Coronavirus. *Nat Commun* 11: 3718. doi:10.1038/s41467-020-17496-8
- [3] World Health Organization. WHO Coronavirus Disease (COVID-19) dashboard.
<https://covid19.who.int/>. Accessed 19 February 2021.
- [4] Richman D (2020) Antiviral drug discovery to address the COVID-19 pandemic. *mBio* 11.
doi:10.1128/mBio.02134-20
- [5] Shahzad F, Anderson D, Najafzadeh M (2020) The antiviral, anti-inflammatory effects of natural medicinal herbs and mushrooms and SARS-CoV-2 infection. *Nutrients* 12:
2573. doi:10.3390/nu12092573
- [6] Davies JP, Almasy KM, McDonald EF, Plate L (2020) Comparative multiplexed interactomics of SARS-CoV-2 and homologous coronavirus non-structural proteins identifies unique and shared host-cell dependencies. *bioRxiv*. doi:10.1101/2020.07.13.201517
- [7] Astuti I, Ysrafil (2020) Severe acute respiratory syndrome coronavirus 2 (SARS-CoV-2): An overview of viral structure and host response. *Diabetes Metab Syndr* 14: 407-412.
doi:10.1016/j.dsx.2020.04.020

- [8] Gil C, Ginex T, Maestro I, Nozal V, Barrado-Gil L, Cuesta-Geijo MÁ. *et al.* (2020) COVID-19: Drug targets and potential treatments. *J Med Chem* 63:12359-12386.
doi:10.1021/acs.jmedchem.0c00606
- [9] Forrestall K, Burley D, Cash M, Pottie I, & Darvesh S (2020) 2-Pyridone natural products as inhibitors of SARS-CoV-2 main protease. *Chem Biol Interact* 109348.
doi:10.1016/j.cbi.2020.109348
- [10] Notarte KI, Devanadera MK, Mayor AB, Cada MC, Pecundo MH, Macabeo AP (2019) Toxicity, antibacterial, and antioxidant activities of fungal endophytes *Colletotrichum* and *Nigrospora* spp. isolated from *Uvaria grandiflora*. *Philipp J Sci* 148: 503-510.
- [11] Quimque MTJ, Notarte KIR, Letada A, Fernandez RAT, Pueblos KRS, Pilapil DYH *et al.* (2020) Antiproliferative, cholinesterase and phosphodiesterase inhibitory activity of the DCM sub-extract of *Uvaria alba*: *In vitro* and *in silico* perspectives [pre-print]. *ChemRxiv*.
doi:10.26434/chemrxiv.12924980.v2
- [12] Elzupir AO (2020) Inhibition of SARS-CoV-2 main protease 3CLpro by means of α -ketoamide and pyridone-containing pharmaceuticals using *in silico* molecular docking. *J Mol Struct* 128878. doi:10.1016/j.molstruc.2020.128878
- [13] Fakhari Z, Faramarzi B, Pacifico S, Faramarzi S (2020) Anthocyanin derivatives as potent inhibitors of SARS-CoV-2 main protease: An in-silico perspective of therapeutic targets against COVID-19 pandemic. *J Biomol Struct Dyn*: 1–13. doi:10.1080/07391102.2020.1801510
- [14] Gentile D, Patamia V, Scala A, Sciortino MT, Piperno A, Rescifina A (2020) Putative inhibitors of SARS-CoV-2 main protease from a library of marine natural products: A virtual screening and molecular modeling study. *Mar drugs* 18: 225. doi:10.3390/md18040225

- [15] Khan A, Khan M, Saleem S, Babar Z, Ali A, Khan AA. *et al.* (2020) Phylogenetic analysis and structural perspectives of RNA-Dependent RNA-Polymerase inhibition from SARS-CoV-2 with natural products. *Interdiscip Sci* 12: 335–348. doi:10.1007/s12539-020-00381-9
- [16] Quimque MTJ, Notarte KIR, Fernandez RAT, Mendoza MAO, Liman RAD. *et al.* (2020) Virtual screening-driven drug discovery of SARS-CoV2 enzyme inhibitors targeting viral attachment, replication, post-translational modification and host immunity evasion infection mechanisms. *J Biomol Struct Dyn* 16: 1-18. doi:10.1080/07391102.2020.1776639
- [17] Zahran EM, Albohy A, Khalil A, Ibrahim AH, Ahmed HA, El-Hossary EM. *et al.* (2020) Bioactivity potential of marine natural products from Scleractinia-associated microbes and in silico anti-SARS-COV-2 evaluation. *Mar Drugs* 18: 645. doi:10.3390/md18120645
- [18] Pettersen EF, Goddard TD, Huang CC, Couch GS, Greenblatt DM, Meng EC. *et al.*, (2004) UCSF Chimera-A visualization system for exploratory research and analysis. *J Comput Chem* 25: 1605–1612. doi:10.1002/jcc.20084
- [19] Yoshimoto FK (2020) The proteins of Severe Acute Respiratory Syndrome Coronavirus-2 (SARS CoV-2 or n-COV19), the cause of COVID-19. *Protein J* 39: 198-216. doi: 10.1007/s10930-020-09901-4
- [20] Gorbalenya AE, Koonin EV, Donchenko AP, Blinov VM (1989) Coronavirus genome: Prediction of putative functional domains in the non-structural polyprotein by comparative amino acid sequence analysis. *Nucleic Acids Res* 17: 4847-4861. doi:10.1093/nar/17.12.4847
- [21] Seybert A, Hegyi A, Siddell SG, Ziebuhr J (2000) The human coronavirus 229E superfamily 1 helicase has RNA and DNA duplex-unwinding activities with 5'-to-3' polarity. *RNA* 6: 1056-1068. doi:10.1017/s1355838200000728

[22] van Dinten LC, van Tol H, Gorbalenya AE, Snijder EJ (2000) The predicted metal-binding region of the arterivirus helicase protein is involved in subgenomic mRNA synthesis, genome replication, and virion biogenesis. *J Virol* 74: 5213-5223. doi:10.1128/jvi.74.11.5213-5223.2000

[23] Chinsembu KC (2019) Chemical diversity and activity profiles of HIV-1 reverse transcriptase inhibitors from plants. *Rev Bras Farmacogn* 29: 504-528. doi:10.1016/j.bjp.2018.10.006

[24] Hanwell MD, Curtis DE, Lonie DC, Vandermeersch T, Zurek E, Hutchison GR (2012) Avogadro: An advanced semantic chemical editor, visualization, and analysis platform. *J Cheminformatics* 4: 17. doi:10.1186/1758-2946-4-17

[25] Wang J, Wang W, Kollman PA, Case DA (2006) Automatic atom type and bond type perception in molecular mechanical calculations. *J Mol Graph Model* 25: 247-260. doi:10.1016/j.jmgm.2005.12.005

[26] Yang J, Roy A, Zhang Y (2013) Protein-ligand binding site recognition using complementary binding-specific substructure comparison and sequence profile alignment. *Bioinformatics* 29: 2588-2595. doi:10.1093/bioinformatics/btt447

[27] Macabeo APG, Cruz AJC, Narmani A, Arzanlou M, Babai-Ahari A, Pilapil LAE *et al.* (2020) Tetrasubstituted α -pyrone derivatives from the endophytic fungus, *Neurospora udagawae*. *Phytochem Lett* 35: 147–151. doi:10.1016/j.phytol.2019.11.010

[28] Phukhamsakda C, Macabeo APG, Huch V, Cheng T, Hyde KD, Stadler M. (2019) Sparticolins A-G, biologically active oxidized spirodioxynaphthalene derivatives from the ascomycete *Sparticola junci*. *J Nat Prod* 82: 2878–2885. doi:10.1021/acs.jnatprod.9b00604

- [29] Mirza MU, Froeyen M (2020) Structural elucidation of SARS-CoV-2 vital proteins: Computational methods reveal potential drug candidates against main protease, Nsp12 polymerase and Nsp13 helicase. *J Pharm Anal* 10: 320-328. doi:10.1016/j.jpha.2020.04.008
- [30] Gao Y, Yan L, Huang Y, Liu F, Zhao Y, Cao L. *et al.* (2020) Structure of the RNA-dependent RNA polymerase from COVID-19 virus. *Science* 368: 779–782. doi:10.1126/science.abb7498
- [31] White MA, Lin W, Cheng X (2020) Discovery of COVID-19 inhibitors targeting the SARS-CoV2 nsp13 helicase. *J Phys Chem Lett* 11: 9144-9151. doi:10.1021/acs.jpcclett.0c02421
- [32] Encinar JA, Menendez JA (2020) Potential drugs targeting early innate immune evasion of SARS-Coronavirus 2 via 2'-O-methylation of viral RNA. *Viruses* 12: 525. doi:10.3390/v12050525
- [33] Krishnan DA, Sangeetha G, Vajravijayan S, Nandhagopal N, Gunasekaran K (2020) Structure-based drug designing towards the identification of potential anti-viral for COVID-19 by targeting endoribonuclease NSP15. *Inform Med Unlocked* 20; 100392. doi:10.1016/j.imu.2020.100392
- [34] Wu C, Liu Y, Yang Y, Zhang P, Zhong W, Wang Y. *et al.* (2020) Analysis of therapeutic targets for SARS-CoV-2 and discovery of potential drugs by computational methods. *Acta Pharm Sin B* 10: 766-788. doi:10.1016/j.apsb.2020.02.008
- [35] Wu A, Peng Y, Huang B, Ding X, Wang X, Niu P. *et al.* (2020) Genome Composition and divergence of the novel coronavirus (2019-nCoV) originating in China. *Cell Host Microbe* 27: 325-328. doi:10.1016/j.chom.2020.02.001

- [36] Henderson JA, Verma N, Shen J (2020) Assessment of proton-coupled conformational dynamics of SARS and MERS coronavirus papain-like proteases: Implication for designing broad-spectrum antiviral inhibitors. *J Chem Phys* 153: 115101. doi:10.1063/5.0020458
- [37] Verma N, Henderson JA, Shen J (2020) Proton-coupled conformational activation of SARS Coronavirus main proteases and opportunity for designing small-molecule broad-spectrum targeted covalent inhibitors. *J Am Chem Soc* 142: 21883-21890. doi:10.1021/jacs.0c10770
- [38] Shereen MA, Khan S, Kazmi A, Bashir N, Siddique R (2020) COVID-19 infection: Origin, transmission, and characteristics of human coronaviruses. *J Adv Res* 24: 91-98. doi:10.1016/j.jare.2020.03.005
- [39] Chen J, Malone B, Llewellyn E, Grasso M, Shelton PMM, Olinares PDB *et al.* (2020) Structural basis for helicase-polymerase coupling in the SARS-CoV-2 replication-transcription complex. *Cell* 182: 1560-1573. doi:10.1016/j.cell.2020.07.033
- [40] Rosas-Lemus M, Minasov G, Shuvalova L, Inniss NL, Kiryukhina O, Brunzelle J. *et al.* (2020) High-resolution structures of the SARS-CoV-2 2'-O-methyltransferase reveal strategies for structure-based inhibitor design. *Sci Signal* 13. doi:10.1126/scisignal.abe1202
- [41] Bhardwaj K, Sun J, Holzenburg A, Guarino LA, Kao CC (2006) RNA recognition and cleavage by the SARS coronavirus endoribonuclease. *J Mol Biol* 361: 243-256. doi:10.1016/j.jmb.2006.06.021
- [42] Deng X, Hackbart M, Mettelman RC, O'Brien A, Mielech AM, Yi G, *et al.* (2017) Coronavirus nonstructural protein 15 mediates evasion of dsRNA sensors and limits apoptosis in macrophages. *Proc Natl Acad Sci USA* 114: E4251-E4260. doi:10.1073/pnas.1618310114
- [43] Fernandez RAT, Quimque MTJ, Notarte KIR, Manzano JAH, Pilapil DYH, de Leon VNO, San Jose JJP, Villalobos OA, Macabeo APG (2021) Myxobacterial depsipeptide chondramides

interrupt SARS-CoV-2 entry by targeting its broad, cell tropic spike protein: Antagonistic prospects for anti-COVID-19 drug discovery [pre-print]. ChemRxiv.

doi:10.26434/chemrxiv.14043641.v1.

[44] Könnnyü B, Sadiq SK, Turányi T, Hírmondó R, Müller B, Kräusslich H. *et al.* (2013) Gag-Pol processing during HIV-1 virion maturation: A systems biology approach. Plos Comput Biol 9: e1003103. doi:10.1371/journal.pcbi.1003103

[45] Subbaraman N (2020) Who gets a COVID vaccine first? Access plants are taking shape Nature 585: 492-493. doi:10.1038/d41586-020-02684-9

[46] He Z, Xia W, Chen J (2008) Isolation and structure elucidation of phenolic compounds in Chinese olive (*Canarium album* L.) fruit. Eur Food Res Technol 226: 1191-1196. doi:10.1007/s00217-007-0653-5

[47] Emade Kwene C, Tih AE, Abderamane B, Ghogomu RT (2020) Two new phenolic glycosides from the leaves of *Garcinia epunctata* Stapf. Z Naturforsch C J Biosci 75: 51–56. doi:10.1515/znc-2018-0217

[48] Singh B, Singh JP, Kaur A, Singh N (2018) Phenolic compounds as beneficial phytochemicals in pomegranate (*Punica granatum* L.) peel: A review. Food Chem 261: 75–86. doi:10.1016/j.foodchem.2018.04.039

[49] Acuña UM, Figueroa M, Kavalier A, Jancovski N, Basile MJ, Kennelly EJ (2010) Benzophenones and biflavonoids from *Rheedia edulis*. J Nat Prod 73: 1775–1779. doi:10.1021/np100322d

[50] Shrestha S, Park J-H, Lee D-Y, Cho J-G, Seo W-D, Kang HC. *et al.* (2012) Cytotoxic and neuroprotective biflavonoids from the fruit of *Rhus parviflora*. J Appl Bio Chem 55: 557–562. doi:10.1007/s13765-012-2090-9

[51] Zhang GG, Jing Y, Zhang HM, Ma EL, Guan J, Xue FN. et al. (2012) Isolation and cytotoxic activity of selaginellin derivatives and biflavonoids from *Selaginella tamariscina*. *Planta Med* 78: 390-392. doi:10.1055/s-0031-1298175

[52] McMahon JB, Currens MJ, Gulakowski RJ, Buckheit RW, Jr Lackman-Smith C, Hallock YF. et al. (1995) Michellamine B, a novel plant alkaloid, inhibits human immunodeficiency virus-induced cell killing by at least two distinct mechanisms. *Antimicrob Agents Chemother* 39: 484–488. doi:10.1128/aac.39.2.484

[53] Senanayake SL (2020) Overcoming nonstructural protein 15-nidoviral uridylyate-specific endoribonuclease (nsp15/NendoU) activity of SARS-CoV-2. *Future Drug Discov* 2. doi:10.4155/fdd-2020-0012

[54] Doak BC, Over B, Giordanetto F, Kihlberg J (2014) Oral druggable space beyond the rule of 5: Insights from drugs and clinical candidates. *Chem Biol* 21: 1115-1142. doi:10.1016/j.chembiol.2014.08.013

[55] Tyagi M, Begnini F, Poongavanam V, Doak BC, Kihlberg J (2020) Drug syntheses beyond the rule of 5. *Chemistry* 26: 49-88. doi:10.1002/chem.201902716

[56] Daina A, & Zoete V (2016) A BOILED-Egg to predict gastrointestinal absorption and brain penetration of small molecules. *ChemMedChem* 11: 1117–1121. doi:10.1002/cmdc.201600182